

## Structures and Isomerization of $\text{LaC}_n^+$ Clusters

Konstantin B. Shelimov, David E. Clemmer, and Martin F. Jarrold\*

Department of Chemistry, Northwestern University, 2145 Sheridan Road, Evanston, Illinois 60208

Received: March 22, 1995; In Final Form: May 16, 1995<sup>⊗</sup>

Injected ion drift tube techniques have been used to examine the structures and to study the isomerization of  $\text{LaC}_n^+$  ( $n = 2-90$ ) clusters. Three families of metal-containing carbon rings ("ring Ia", "ring Ib", and "ring II"), metal-containing graphite sheets, and metallofullerenes have been resolved. Several plausible geometries with similar mobilities can be suggested for all of the ring isomers. The most likely geometries are a La inserted into a carbon ring (ring Ia), a La inside a carbon ring (ring Ib), and various  $\text{LaC}_n$  and  $\text{C}_m$  rings fused together (ring II). The relative abundances of the graphite sheet and the metallofullerene isomers are substantially larger than for the pure carbon clusters. Both endohedral and non-endohedral  $\text{LaC}_n^+$  metallofullerenes have been resolved.  $\text{LaC}_{36}^+$  and all  $\text{LaC}_n^+$  fullerenes with  $n = 38-90$  are found to be endohedral, while  $\text{LaC}_{29}^+ - \text{LaC}_{35}^+$  fullerenes are non-endohedral. Annealing studies show that  $\text{LaC}_n^+$  ring II isomers with an even number of carbon atoms convert into ring Ia isomers, while the odd-numbered ring II isomers convert into ring Ib isomers. For larger clusters, fullerenes and graphite sheets are formed when the rings are annealed. The efficiency of this annealing process in the  $\text{LaC}_n^+$  system is much larger than in the  $\text{C}_n^+$  system, although the activation energies appear to be approximately the same. Studies of the dissociation of  $\text{LaC}_n^+$  show that loss of  $\text{LaC}_4^+$  is generally the dominant dissociation process for the  $\text{LaC}_n^+$  rings with an even number of carbon atoms, while loss of  $\text{C}_3$  is also important for the odd-numbered ones.

### Introduction

Since the original discovery of fullerenes (closed, roughly spherical carbon networks<sup>1</sup>) and endohedral metallofullerenes (fullerene cages encapsulating metal atoms<sup>2</sup>), a vast research effort has been devoted to these interesting and potentially useful species.<sup>3</sup> A variety of pure carbon fullerenes<sup>4</sup> and metallofullerenes<sup>5</sup> as well as other forms of carbon networks such as multiwall tubules,<sup>6</sup> nanotubes,<sup>7</sup> and polyhedra<sup>8</sup> have been synthesized and studied. The availability of macroscopic quantities of some of these species has made possible structural analysis using such techniques as EPR,<sup>9</sup> XPS,<sup>10</sup> and EXAFS.<sup>11</sup> One of the problems impeding studies of the physics and chemistry of fullerenes and metallofullerenes is that only a limited number of them (such as, for example,  $\text{C}_{60}$ ,  $\text{C}_{70}$ ,  $\text{C}_{74}$ , and  $\text{C}_{84}$  for pure fullerenes<sup>4,12</sup> and  $\text{LaC}_{82}$  for La-doped fullerenes<sup>5,13</sup>) are available in a pure form in sufficiently large quantities for detailed studies with a wide range of analytical techniques. If the properties of a wide variety of fullerenes or metallofullerenes are of interest, one has to resort to gas phase studies, where these species can be easily produced and mass-selected.

A question that often arises in studies of metallofullerenes concerns the location of the metal atom (or atoms) with respect to the carbon cage. Metallofullerenes produced using arc generation methods are usually assumed to be endohedral, although direct evidence for this is scarce. Studies of Y-containing fullerenes using a structurally sensitive technique such as EXAFS have given contradicting results about the position of metal atoms.<sup>11</sup> In the gas phase, information about the location of the metal atom is generally obtained from indirect indicators, such as the dissociation pattern and chemical reactivity.<sup>14,15</sup>

Mobility measurements are currently the most direct method for determining the structures of medium-sized clusters in the gas phase.<sup>16</sup> This method utilizes the fact that the mobility of

a gas phase ion depends on its geometry. Thus, structural isomers can be separated on the basis of their different mobilities, and the measured mobilities can be used to obtain information about cluster geometries. The use of mobilities to separate structural isomers of gas phase ions was first demonstrated using ion mobility spectrometry,<sup>17</sup> a drift-tube-based analytical technique developed in the early 1970s.<sup>18</sup> This technique was originally called plasma chromatography, but the name was changed to avoid confusion because the separation that occurs in a drift tube is not chromatography.<sup>19</sup> Ion mobility measurements provide especially useful information when applied to clusters of atoms with highly directional bonding such as carbon<sup>20</sup> or silicon.<sup>21</sup> An extensive study of carbon cluster geometries performed by von Helden *et al.*<sup>20</sup> showed that carbon exists in the gas phase in a variety of isomers, including mono-, bi-, and polycyclic rings and fullerenes. Ion mobility measurements can also be used to study isomer interconversion. Specifically, Hunter *et al.*<sup>22,23</sup> demonstrated that vibrationally excited bi- and polycyclic carbon rings can isomerize into fullerenes with a relatively low activation barrier (around 2.4 eV for  $\text{C}_{60}$ ).

Recently, we have undertaken a series of studies of metal-containing carbon clusters, including  $\text{LaC}_n^+$ <sup>24-26</sup> and  $\text{NbC}_n^+$ .<sup>27</sup> The purpose of these studies is to determine how the presence of the metal atom affects the nature of the isomers that are present and the interconversion of the observed isomers. For the fullerenes, determining the position of the metal atom (endohedral or exohedral) is of particular interest. The effect of the metal atom on the isomerization of metal-containing carbon rings into metallofullerenes is also an important issue. Some of the results of our studies of La-containing carbon clusters have been reported previously.<sup>24-26</sup> In this paper we present the results of ion mobility measurements of  $\text{LaC}_n^+$  clusters with 2–90 carbon atoms, along with the results of annealing and fragmentation studies for all of the observed  $\text{LaC}_n^+$  isomers.

<sup>⊗</sup> Abstract published in *Advance ACS Abstracts*, July 1, 1995.

## Experimental Methods

The experimental apparatus used in the present study has been described in detail previously.<sup>28,29</sup> In brief, metal-containing carbon cluster cations are generated by pulsed laser vaporization of a composite  $\text{LaC}_2$ /graphite rod in a flow of helium buffer gas. The rods were prepared by mixing  $\text{LaC}_2$  (Johnson Matthey, 99%), graphite powder (Johnson Matthey, 99.9995%), and graphite cement (Dylon Industries, GC grade) in a 1:60 La:C molar ratio and subsequent baking at 1000 °C for about 1 day. Cluster ions that exit the source are mass-selected with a quadrupole mass spectrometer and injected into a drift tube containing around 5 Torr of helium buffer gas. The injection energy can be varied from 5 eV up to around 400 eV. As the ions enter the drift tube, a fraction of their kinetic energy is converted into internal energy through collisions with the buffer gas. If the injection energy (and thus the internal energy deposited into a cluster through collisions) is large enough, the cluster may isomerize or fragment. Further collisions with the buffer gas cool the clusters to thermal energies. The clusters then drift slowly across the drift tube under the influence of a weak (13.1 V/cm) electric field. Upon exiting the drift tube, cluster cations are mass-analyzed by the second quadrupole mass spectrometer and detected with an off-axis collision dynode and dual microchannel plates.

Drift time distributions are measured by injecting a short (50  $\mu\text{s}$ ) pulse of size-selected clusters into the drift tube and recording the arrival time distribution at the detector with a multichannel analyzer. Drift times are obtained by subtracting the arrival time measured without the buffer gas in the drift tube (plus some small corrections to the time scale) from the arrival times measured with the buffer gas in the drift tube. The drift time distributions provide information about the number of structural isomers present, their relative abundances, and their mobilities in the He buffer gas. Reduced mobilities are obtained using the expression

$$K_0 = \frac{L}{t_D} \frac{P}{E} \frac{273.2}{T} \quad (1)$$

where  $L$  is the length of the drift tube,  $t_D$  is the drift time,  $E$  is the electric field,  $P$  is the pressure of the buffer gas in Torr, and  $T$  is the buffer gas temperature in kelvin. The reduced mobilities of various isomers are used to obtain information about their structures, as discussed below.

## Results

**1. Isomer Distributions.** Figure 1 shows examples of drift time distributions recorded for  $\text{LaC}_n^+$  clusters with 6, 16, 26, 36, and 46 carbon atoms. Several isomers are resolved in most of these distributions. Figure 2 shows the inverse mobilities of these isomers plotted against cluster size. This plot shows that the observed isomers fall into five distinct families. One can obtain information about the general shapes of these isomers by comparing their mobilities with those previously measured for pure  $\text{C}_n^+$  clusters<sup>20,30</sup> (which are plotted as the solid lines in Figure 2). The  $\text{C}_n^+$  isomers are (in order of their appearance with increasing cluster size) linear chains, monocyclic rings, bicyclic rings, graphite sheets, and fullerenes.<sup>20,31</sup> The inverse mobilities of  $\text{C}_n^+$  and  $\text{LaC}_n^+$  isomers increase roughly linearly with cluster size, and the differences in the slopes of these linear dependencies reflect different cluster growth sequences. The three slowest isomers of  $\text{LaC}_n^+$  have mobilities that roughly parallel those of the  $\text{C}_n^+$  mono- and bicyclic rings, indicating that these three isomers follow ringlike growth sequences. We therefore assign these isomers (labeled "ring Ia", "ring Ib", and

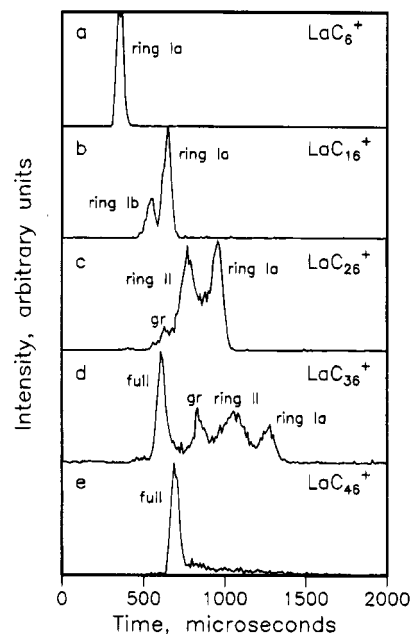


**Figure 1.** Drift time distributions of some  $\text{LaC}_n^+$  clusters recorded at low (50 eV) injection energy. Almost no isomerization or dissociation of  $\text{LaC}_n^+$  clusters is observed at this injection energy, so that the drift time distributions reflect the relative abundances of isomers coming directly from the source. The structures observed are the three ring isomers (labeled "ring Ia", "ring Ib", and "ring II"), metal-containing graphite sheets (labeled "gr"), and metallofullerenes (labeled "full").

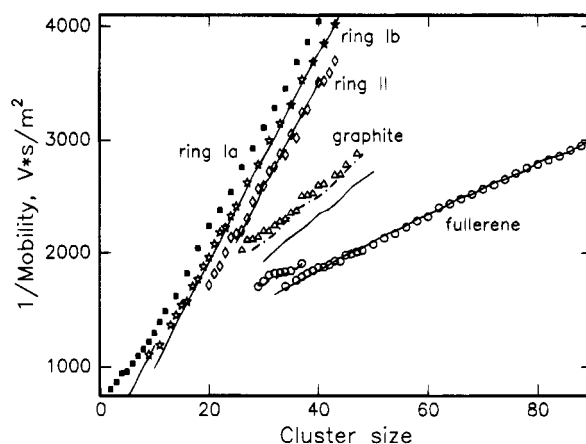


**Figure 2.** Plot of the inverse mobilities of  $\text{LaC}_n^+$  isomers against the cluster size (points). The solid lines show the mobilities of pure  $\text{C}_n^+$  clusters.<sup>20,30</sup> The  $\text{C}_n^+$  isomers are (in order of their appearance with increasing cluster size) linear chains, monocyclic rings, bicyclic rings, graphite sheets, and fullerenes. The dashed line shows the calculated mobilities of networked  $\text{LaC}_n^+$  metallofullerenes and the dashed-dotted line shows the calculated mobilities of metal-containing graphite sheets (see text).

"ring II" in Figures 1 and 2) to La-containing carbon rings. Two other  $\text{LaC}_n^+$  isomers have mobilities that roughly parallel those of  $\text{C}_n^+$  graphite sheets and fullerenes, and these are assigned to metal-containing graphite sheets and metallofullerenes, respectively. A detailed discussion of possible structures for all five  $\text{LaC}_n^+$  isomers is given below.

Ring Ia is the only  $\text{LaC}_n^+$  isomer observed for clusters with 2–8 carbon atoms. In this size range, linear chains are the dominant isomer for pure  $\text{C}_n^+$  clusters.<sup>20</sup> As is apparent from Figure 2, the variation in the mobility of linear chains with cluster size (the solid line for clusters with 3–10 atoms) is larger than that observed for  $\text{LaC}_n^+$  ring Ia. We are therefore confident that even small isomers from the ring Ia family are

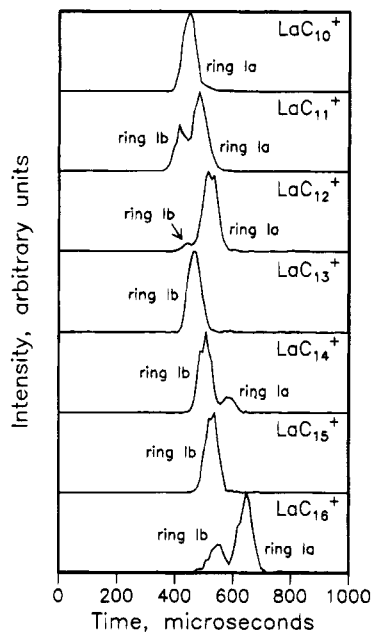


**Figure 3.** Drift time distributions for  $\text{LaC}_n^+$  ( $n = 10-16$ ) clusters recorded at 100 eV injection energy.

indeed ringlike structures and not linear chains (with the possible exception of  $\text{LaC}_2^+$  and  $\text{LaC}_3^+$ ).

Ring Ib first appears for  $\text{LaC}_9^+$  as a shoulder on the ring Ia peak and for  $\text{LaC}_{11}^+$  as a separate well-resolved peak. Starting at this cluster size, the relative abundances of ring Ia and ring Ib show pronounced odd-even alterations: ring Ia tends to be more abundant for  $\text{LaC}_n^+$  clusters with an even number of carbon atoms, while ring Ib dominates for clusters with an odd number of carbon atoms (see Figure 3). For all  $\text{LaC}_{2n+1}^+$  clusters with more than 12 carbon atoms the abundance of ring Ia is essentially zero (see Figure 3). The ring Ib isomer can be resolved in the drift time distributions for  $\text{LaC}_{2n}^+$  clusters up to  $\text{LaC}_{24}^+$ . For larger  $\text{LaC}_{2n}^+$  clusters ring Ib is not resolved from the broader ring II peak (see Figure 1c).

Ring II first appears for  $\text{LaC}_{20}^+$  and becomes the dominant isomer in unannealed isomer distributions around  $\text{LaC}_{27}^+$  (see Figure 1c). Unlike ring Ia and ring Ib, ring II shows no pronounced odd-even variations in relative abundance. The width of the ring II peak in the drift time distributions, however, does exhibit an odd-even variation. The widths of ring II peaks for  $\text{LaC}_n^+$  clusters with an even number of carbon atoms are 2–2.5 times larger than those calculated from the gas phase ion transport equation<sup>32</sup> assuming the existence of only one ring II structure. This indicates that at least two different  $\text{LaC}_n^+$  ring II structures are present. The widths of ring II peaks for  $\text{LaC}_{2n+1}^+$  clusters are about 1.5 times larger than the calculated ones, which may be due to small variations in geometry of one structural isomer.

For  $\text{LaC}_n^+$  ( $n \geq 33$ ) clusters a new isomer (or a group of isomers) with the drift times slightly smaller than those for ring II starts to emerge. This isomer appears as a shoulder on the ring II peak (see Figure 1d) and cannot be resolved as a separate peak. Its relative abundance does not exceed 10%. A similar feature in drift time distributions of pure  $\text{C}_n^+$  clusters in this size range has been attributed to the appearance of polycyclic carbon rings.<sup>20</sup> We therefore believe that this new peak corresponds to another ring isomer, although the resolution of our instrument does not allow us to obtain any detailed information about its structure.

Metal-containing graphite sheets are first observed in the drift time distributions at  $\text{LaC}_{26}^+$  (see Figure 1c). Their relative

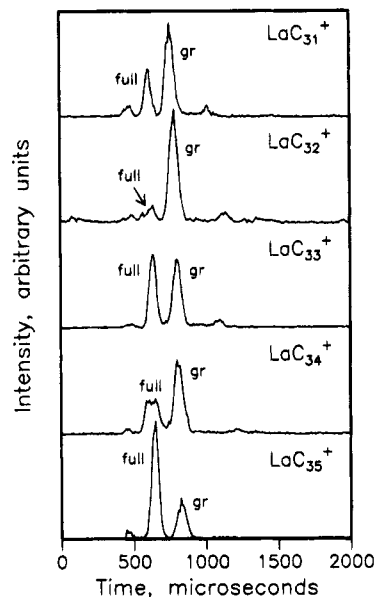


**Figure 4.** Drift time distributions for  $\text{LaC}_n^+$  ( $n = 31-35$ ) clusters recorded at 250 eV injection energy. The two main isomers seen in these distributions are the graphite sheet (labeled “gr”) and the metallofullerene (labeled “full”). At this injection energy the ring isomers have either dissociated or annealed into the fullerene and the graphite sheet. Two fullerene isomers (endohehedral and non-endohehedral) with slightly different drift times can be clearly seen for  $\text{LaC}_{34}^+$ . The low-intensity features with slightly shorter drift times than the fullerene probably result from doubly charged clusters.

abundance sharply increases between  $\text{LaC}_{26}^+$  and  $\text{LaC}_{32}^+$ , so that they are the dominant isomer for clusters with 30–34 carbon atoms, but then starts to decline. The smallest metallofullerene is observed at  $\text{LaC}_{29}^+$ . Metallofullerenes become the dominant isomer for  $\text{LaC}_{35}^+$  and larger clusters (see Figure 1d). For  $\text{LaC}_{2n}^+$  clusters larger than  $\text{LaC}_{40}^+$  the fullerene isomer comprises more than 50% of the isomer population (the relative abundances of the fullerene and non-fullerene isomers depend somewhat on the source conditions). The metallofullerene is the only isomer that can be clearly resolved in the drift time distributions of the larger clusters (see Figure 1e). The broad distribution of non-fullerene isomers observed in this size range probably consists of metal-containing polycyclic rings and possibly graphite-like (and bowl-like) structures.

An abrupt change in the mobility of  $\text{LaC}_n^+$  metallofullerenes is observed around  $\text{LaC}_{36}^+$  (see Figure 2). The mobilities of  $\text{LaC}_n^+$  ( $n = 29-33$  and 35) metallofullerenes are 8–12% smaller than the mobilities of  $\text{C}_n^+$  fullerenes of the same size, while the mobilities of  $\text{LaC}_{36}^+$ ,  $\text{LaC}_{38}^+$ , and all larger metallofullerenes are essentially identical to those of  $\text{C}_n^+$  fullerenes. For  $\text{LaC}_{34}^+$  and  $\text{LaC}_{37}^+$  we observe two fullerene isomers with mobilities that differ by about 10% (Figure 4). All  $\text{LaC}_n^+$  metallofullerenes show a pronounced odd-even variation in relative abundances. For  $\text{LaC}_n^+$  with  $n \geq 36$ , metallofullerenes with an even number of carbon atoms are more abundant, which is typical for pure  $\text{C}_n$  fullerenes and endohedral metallofullerenes. In contrast, for  $\text{LaC}_n^+$  ( $n = 29-35$ ) clusters, metallofullerenes with an odd number of carbon atoms are more abundant (see Figure 4). We attribute these differences in the mobilities and the relative abundances of  $\text{LaC}_n^+$  metallofullerenes to differences in the position of the metal atom with respect to a carbon cage, as discussed in more detail below.

The results presented above show that  $\text{C}_n^+$  and  $\text{LaC}_n^+$  clusters have similar basic structural isomers. However, the metal atom has a significant effect on the relative abundances of these isomers. This effect is illustrated in Figure 5a,d by comparing

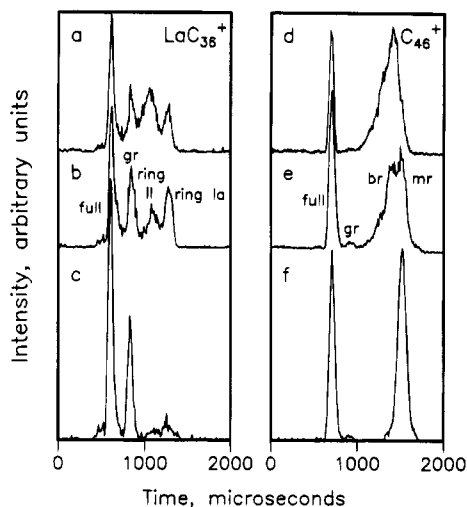


**Figure 5.** Normalized drift time distributions for  $\text{LaC}_{36}^+$  and  $\text{C}_{46}^+$  recorded at injection energies of 50 eV (a and d), 150 eV (b and e), and 225 eV (c and f). The  $\text{LaC}_{36}^+$  isomer labeling is the same as in Figure 1. "mr" and "br" labels indicate  $\text{C}_{46}^+$  mono- and bicyclic rings, respectively. The broad feature at longer drift times observed for  $\text{C}_{46}^+$  at 50 eV consists of unresolved mono-, bi-, and tricyclic rings.

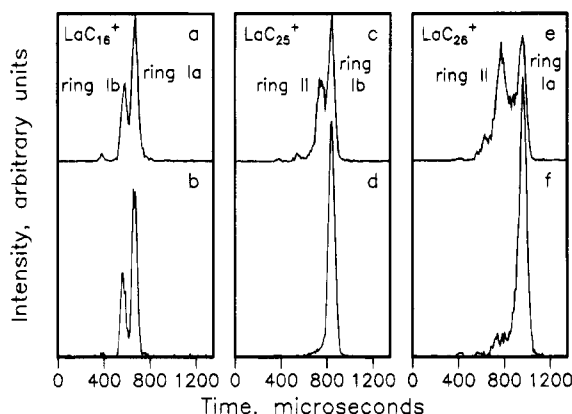


**Figure 6.** Normalized drift time distributions for  $\text{LaC}_{16}^+$ ,  $\text{LaC}_{25}^+$ , and  $\text{LaC}_{26}^+$ . The distributions were recorded at injection energies of (a) 50, (b) 150, (c) 50, (d) 125, (e) 40, and (f) 140 eV.

isomer distributions for  $\text{LaC}_{36}^+$  and  $\text{C}_{46}^+$ . For  $\text{C}_{46}^+$  the broad feature at long drift times (consisting of mono-, bi-, and polycyclic carbon rings) dominates the isomer distribution at low injection energies, while the combined relative abundance of the graphite sheet and the fullerene is around 20%. On the other hand, the metallofullerene and the metal-containing graphite sheet account for more than 50% of the isomer distribution for  $\text{LaC}_{36}^+$ , despite the fact that the abundance of these isomers is normally smaller for smaller clusters. The increase in the relative abundances of the fullerene and the graphite sheet isomers compared to the  $\text{C}_n^+$  system is observed for all  $\text{LaC}_n^+$  ( $n \geq 30$ ) clusters.

**2. Annealing of the Isomer Distributions.** When the injection energy is increased, the transient heating that occurs as the clusters enter the drift tube can become large enough to induce annealing of the isomer distribution. The two major types of annealing processes observed for  $\text{LaC}_n^+$  clusters are interconversion of the ring isomers and isomerization of the rings into metallofullerenes and graphite sheets. Interconversion of  $\text{LaC}_n^+$  rings is illustrated in Figure 6. For  $\text{LaC}_{2n}^+$  clusters with up to 22 carbon atoms the two major ring isomers observed in drift time distributions are ring Ia and ring Ib (see Figure 6a). Comparison of drift time distributions for  $\text{LaC}_{16}^+$  at injection energies of 50 and 150 eV (Figure 6a,b) shows that the relative abundances of these two isomers are essentially

independent of injection energy. Similar behavior is observed for the ring Ia and ring Ib isomers for all  $\text{LaC}_{2n}^+$  ( $2n = 14-22$ ) clusters. An injection energy of 150 eV is more than enough to drive isomerization processes in slightly larger pure  $\text{C}_n^+$  clusters. The fact that the relative abundance of ring Ia and ring Ib remains unchanged at these high injection energies indicates that either ring Ia and ring Ib do not interconvert or the interconversion rates in both directions are equal. In the first case the activation barrier for interconversion must be very high, while in the second case it must be low enough so that the relative abundances of ring Ia and ring Ib generated by the source already reflect the equilibrium values. Since ring Ia and ring Ib are expected to have similar structures (they are both ring isomers), it seems more likely that they interconvert easily and that their relative abundances for  $\text{LaC}_{2n}^+$  ( $2n = 14-22$ ) clusters reflect an equilibrium. This conclusion is supported by recent laser annealing studies performed in our laboratory. This new experimental approach, which permits individual structural isomers to be annealed with a pulsed laser, will be described in detail in the future.

For  $\text{LaC}_{23}^+$  and larger clusters ring II comprises a significant fraction of the isomer distribution. Figure 6c-f compares isomer distributions for  $\text{LaC}_{25}^+$  and  $\text{LaC}_{26}^+$  at injection energies of 50 and 125–140 eV. The amount of fragmentation at injection energies of 125–140 eV is less than 5%, so that the changes in relative abundances of  $\text{LaC}_n^+$  isomers are due to isomerization processes. It is clear from Figure 6 that the major fraction of ring II isomerizes to form ring Ib (for  $\text{LaC}_{25}^+$ ) or ring Ia (for  $\text{LaC}_{26}^+$ ). A similar process—interconversion of bicyclic rings into monocyclic rings at injection energies around 100 eV—has been previously observed for pure  $\text{C}_n^+$  clusters in this size range<sup>29,31</sup> (see Figure 5, d and e). At an injection energy of 125 eV essentially all of the  $\text{LaC}_{25}^+$  rings II isomerize into ring Ib. For  $\text{LaC}_{26}^+$  the isomerization efficiency at 140 eV is around 80%, and it does not increase with further increase in the injection energy. Isomerization processes similar to those for  $\text{LaC}_{25}^+$  and  $\text{La}_{26}^+$  are observed for all  $\text{LaC}_n^+$  ( $20 \leq n \leq 40$ ) clusters.

As described above, ring Ib is not resolved in the drift time distributions of  $\text{LaC}_{2n}^+$  ( $2n > 24$ ) clusters (see Figure 6e). However, the signal intensity between the ring II and the ring Ia peaks (i.e. in the drift time range corresponding to ring Ib) is not zero so that it is possible that ring Ib still exists for these clusters. Comparison between parts e and f of Figure 6 then implies that ring Ib can now isomerize into ring Ia, since the abundances of all isomers present clearly decrease relative to that of ring Ia with increasing injection energy. This observation suggests that the  $\text{LaC}_{2n}^+$  ring Ib isomer becomes less stable relative to the ring Ia isomer with increasing cluster size.

For  $\text{LaC}_n^+$  ( $n > 30$ ) clusters La-containing graphite sheets and metallofullerenes become abundant. Our annealing studies show that these isomers can be formed through isomerization of metal-containing carbon rings, similar to the processes that have been observed for pure carbon clusters.<sup>22,23</sup> The isomerization processes for  $\text{LaC}_{36}^+$  and  $\text{C}_{46}^+$ <sup>33</sup> are illustrated in Figure 5. For both clusters the ring isomers dominate in the drift time distributions at low injection energies (Figure 5a,d). As the injection energy is increased at 150 eV (Figure 5b,e), the abundances of  $\text{LaC}_{36}^+$  ring II and  $\text{C}_{46}^+$  bicyclic ring decrease, while the abundances of  $\text{LaC}_{36}^+$  ring Ia and  $\text{C}_{46}^+$  monocyclic ring increase (this behavior is similar to the  $\text{LaC}_{26}^+$  case discussed above). The abundances of  $\text{LaC}_{36}^+$  fullerene and graphite sheet at this injection energy are virtually unchanged, while the abundance of  $\text{C}_{46}^+$  fullerene increases slightly. However, as the injection energy is increased to 225 eV, the

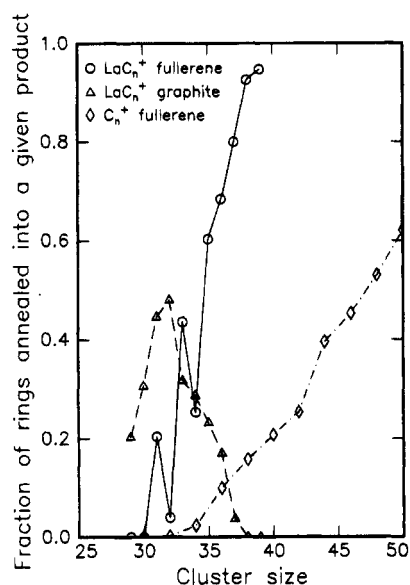


**Figure 7.** Fraction of ring isomers annealed into fullerenes and graphite sheets at injection energies of 225–250 eV. For  $\text{LaC}_{34}^+$  and  $\text{LaC}_{37}^+$  the fractions annealed into endohedral and non-endohedral fullerenes are summed. The absolute uncertainty in the  $\text{LaC}_n^+$  data is around  $\pm 0.05$ . The data for  $\text{C}_n^+$  clusters are taken from ref 23. Essentially no conversion of  $\text{C}_n^+$  rings into graphite sheets has been observed.

abundances of  $\text{LaC}_{36}^+$  fullerene and graphite sheet increase dramatically, and so does the abundance of  $\text{C}_{46}^+$  fullerene (see Figure 5c,f). At this relatively high injection energy some fragmentation (around 5% for  $\text{LaC}_{36}^+$  and 15% for  $\text{C}_{46}^+$ ) is observed, but the changes in the relative abundances of the isomers are still due primarily to the isomerization processes. For  $\text{LaC}_{36}^+$  the abundances of both ring Ia and ring II at 225 eV injection energy are smaller than in the unannealed isomer distribution, i.e. both ring isomers are converted into the fullerene and the graphite sheet. For  $\text{C}_{46}^+$ , however, the abundance of the monocyclic ring is larger at an injection energy of 225 eV, suggesting that this isomer is not efficiently converted into the fullerene. Therefore, the efficiency of fullerene (and graphite sheet) formation for  $\text{LaC}_{36}^+$  is substantially higher than for  $\text{C}_{46}^+$ , despite the fact that the efficiency of this process generally increases with cluster size.

Isomerization processes similar to those discussed above for  $\text{LaC}_{36}^+$  are observed for other  $\text{LaC}_n^+$  ( $n > 30$ ) clusters. The efficiency of the isomerization of rings into fullerenes and graphite sheets for  $\text{LaC}_n^+$  and  $\text{C}_n^+$  clusters is plotted against the cluster size in Figure 7. For  $\text{C}_n^+$  clusters the efficiency of fullerene formation is determined by the branching ratio for isomerization of the bi- and polycyclic carbon rings into the fullerene and the monocyclic ring.<sup>23</sup> This branching ratio slowly increases with cluster size, so that the efficiency of fullerene formation reaches only 60% for  $\text{C}_{50}^+$  (the dashed-dotted line in Figure 7). The conversion of  $\text{C}_n^+$  rings into graphite sheets is insignificant for all cluster sizes. For  $\text{LaC}_n^+$  clusters the efficiency of fullerene formation is determined by the branching ratio for isomerization of rings into fullerenes and dissociation of the rings and sharply increases from essentially zero for  $\text{LaC}_{30}^+$  to more than 90% for  $\text{LaC}_{39}^+$  (the solid line in Figure 7). The isomerization efficiency for  $\text{LaC}_n^+$  ( $n = 30$ –55) rings is larger for clusters with an odd number of carbon atoms, in line with a similar odd–even variation in the relative abundances of metallofullerenes in this size range mentioned above (see Figure 4). The efficiency of rings-to-graphite sheet conversion for  $\text{LaC}_n^+$  clusters rises sharply for  $n = 29$ –32, but then decreases to essentially zero for  $\text{LaC}_{38}^+$  and larger clusters (the dashed line in Figure 7). This suggests that for  $n = 29$ –36

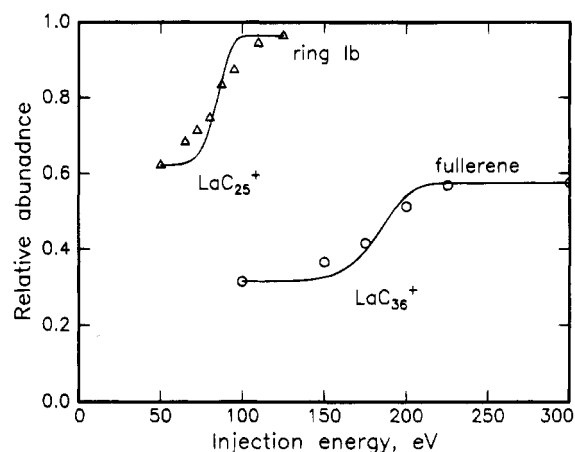


**Figure 8.** Points show the relative abundances of  $\text{LaC}_{25}^+$  ring Ib and  $\text{LaC}_{36}^+$  fullerene as a function of the injection energy. The lines represent the results of the annealing threshold simulations described in the text.

metallofullerenes and graphite sheets have comparable stabilities (at the elevated temperatures where the isomerization occurs) and compete with each other as products of  $\text{LaC}_n^+$  ring isomerization. For larger clusters, metallofullerenes become substantially more stable than graphite sheets, and essentially all the rings now isomerize to form fullerenes.

For several cluster sizes we have performed detailed studies of the annealing processes as a function of the injection energy. The results of these studies for  $\text{LaC}_{25}^+$  and  $\text{LaC}_{36}^+$  are presented in Figure 8. As discussed above, the increase in the relative abundance of  $\text{LaC}_{25}^+$  ring Ib isomer with injection energy is due to the isomerization of ring II, while the increase in the relative abundance of  $\text{LaC}_{36}^+$  fullerene is due to the isomerization of both ring Ia and ring II. An estimate of the activation energy associated with these isomerization processes can be obtained from the data shown in Figure 8 using a simple semiempirical model described previously.<sup>34</sup> The fraction of the ion's injection energy that is converted into the internal energy as the ions enter the drift tube is estimated using a simple modified impulsive collision model<sup>34,35</sup> as

$$F_{ie} = C \frac{1}{N} \sum_{i=1}^N \frac{1 - m_i/M}{1 + m_i/m} \quad (2)$$

where  $C = 0.4$  is an empirical correction factor,  $N$  is the number of atoms in the cluster,  $m_i$  is the mass of the  $i$ th atom,  $M$  is the mass of the cluster, and  $m$  is the mass of a buffer gas atom. The isomerization rate of a vibrationally excited cluster is calculated using RRK theory.<sup>36</sup> The reaction time is assumed to be on the order of the time between collisions with buffer gas atoms. While this model uses many assumptions and we do not expect our estimates to be accurate to more than  $\pm 0.5$  eV, it does provide a useful way to determine how the activation energies for isomerizations in the  $\text{LaC}_n^+$  system compare to those in the  $\text{C}_n^+$  system. The solid lines in Figure 8 show the isomerization thresholds for  $\text{LaC}_{25}^+$  and  $\text{LaC}_{36}^+$  calculated using the model described above. The calculated thresholds are substantially more narrow than the measured ones since our model does not take into account the distribution of internal energies in the excited clusters and the possible existence of several isomers with slightly different isomerization rates. The estimated activation energies for isomerization of ring II into ring Ia and ring Ib and of rings into fullerenes for some  $\text{LaC}_n^+$  clusters are listed in Table 1. The estimated activation energies

**TABLE 1: Estimated Activation Energies for Isomerization of  $\text{C}_n^+$  and  $\text{LaC}_n^+$  Rings (eV)**

cluster	isomerization of ring II into ring Ia and ring Ib	isomerization of rings into fullerenes
$\text{LaC}_{25}^+$	2.2	
$\text{LaC}_{26}^+$	2.2	
$\text{C}_{25}^+$	2.4 <sup>a</sup>	
$\text{C}_{26}^+$	2.4 <sup>a</sup>	
$\text{LaC}_{35}^+$		3.1
$\text{LaC}_{36}^+$		3.1
$\text{C}_{40}^+$		2.8 <sup>b</sup>

<sup>a</sup> The activation energy for isomerization of a bicyclic ring into a monocyclic ring.<sup>31</sup> <sup>b</sup> Reference 23.

are around 2.2 eV for ring-to-ring isomerization and around 3.1 eV for ring-to-fullerene annealing. Both these values are close to those for similar processes in pure carbon clusters.

For  $\text{LaC}_{40}^+$  and larger clusters, separate nonfullerene isomers are not resolved in the drift time distributions (see Figure 1e). The broad distribution of nonfullerene isomers present for these clusters readily anneals into the metallofullerene at injection energies of 150–250 eV.<sup>24</sup>

**3. Dissociation of  $\text{LaC}_n^+$  Clusters.** If  $\text{LaC}_n^+$  clusters are injected into the drift tube with kinetic energies even higher than those discussed above, a significant fraction of the incoming cluster beam dissociates. For  $\text{LaC}_n^+$  ( $n < 30$ ) clusters, the isomer distribution coming from the source consists primarily of rings which almost completely dissociate at injection energies of 250 eV or less. The main dissociation pathway for most of the  $\text{LaC}_{2n}^+$  ( $2n > 4$ ) rings and large ( $2n + 1 > 15$ )  $\text{LaC}_{2n+1}^+$  rings is the loss of  $\text{LaC}_4^+$  (with smaller amounts of other  $\text{LaC}_{2n}^+$ ,  $n = 0-5$ , fragments). For small  $\text{LaC}_{2n+1}^+$  rings, loss of  $\text{C}_3$  (and  $\text{C}_5$ ) is competitive with the loss of  $\text{LaC}_4^+$ . Loss of  $\text{C}_3$  (and  $\text{C}_5$ ) is the main dissociation pathway for pure carbon rings with 10–30 carbon atoms.<sup>37</sup> Loss of any  $\text{LaC}_m^+$  fragment from a  $\text{LaC}_n^+$  ring requires the breaking of the same number of carbon carbon bonds, so the preferential loss of  $\text{LaC}_4^+$  and other  $\text{LaC}_{2m}^+$  fragments from  $\text{LaC}_n^+$  rings must be due to their higher thermochemical stability compared to  $\text{LaC}_{2m+1}^+$  fragments. The loss of  $\text{C}_3$  fragments from  $\text{LaC}_n^+$  rings with an even number of carbon atoms is presumably disfavored because it results in the formation of less stable  $\text{LaC}_{2m+1}^+$  products. Loss of  $\text{C}_3$  from  $\text{LaC}_{2n+1}^+$  rings results in formation of the more stable  $\text{LaC}_{2m}^+$  fragments and therefore can be competitive with the loss of  $\text{LaC}_4^+$ . An enhancement in the formation of certain  $\text{LaC}_{2n}^+$  fragments is observed if the remaining carbon ring has  $4m + 2$  carbon atoms. For example,  $\text{LaC}_{16}^+$  loses predominantly  $\text{LaC}_2^+$  (rather than  $\text{LaC}_4^+$ ) fragments, since this fragmentation process can result in the formation of a stable  $\text{C}_{14}$  ring.

For  $\text{LaC}_n^+$  clusters with 30–40 carbon atoms several isomers are present in the isomer distributions generated by the source, and a substantial fraction of the ring isomers anneals into fullerenes and graphite sheets. The onset of this annealing process is accompanied by a sharp drop in dissociation at the higher injection energies: the amount of fragmentation at the injection energy of 250 eV drops from around 50% for  $\text{LaC}_{30}^+$  to around 8% for  $\text{LaC}_{36}^+$ . This implies that metallofullerenes and metal-containing graphite sheets in the  $\text{LaC}_{30}^+ - \text{LaC}_{40}^+$  size range are more stable toward dissociation than the metal-containing rings. The abundances of the graphite sheets relative to the fullerenes in the drift time distributions remain virtually unchanged at injection energies up to 250 eV (see Figure 5), but start to decrease at higher injection energies. At the same time the amount of fragmentation increases, and the main fragmentation products are again  $\text{LaC}_4^+$  and other  $\text{LaC}_{2n}^+$  fragments. At the present time we cannot determine unambigu-

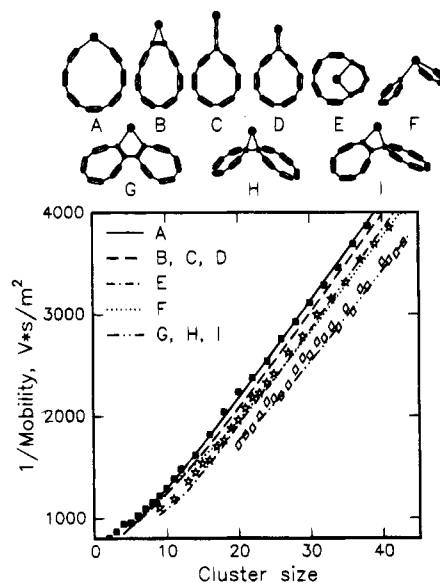


**Figure 9.** Possible geometries resulting from binding a  $\text{La}^+$  ion to carbon rings (see discussion in the text) and their mobilities. The points on the plot are the measured mobilities of  $\text{LaC}_n^+$  rings (filled squares for ring Ia, stars for ring Ib, and diamonds for ring II). The lines show the calculated mobilities of the proposed structures. The calculated mobilities of structures B–D and G–I are essentially identical.

ously whether some of  $\text{LaC}_n^+$  ( $n = 30-40$ ) graphite sheets isomerize to form metallofullerenes. If this process is at all possible, it occurs at injection energies above 250 eV, so that the activation energies must be higher than those for isomerization of the rings into fullerenes.

For  $n \geq 40$  the isomer distribution generated by the source consists primarily of metallofullerenes (see Figure 1e). Large metallofullerenes with an even number of carbon atoms are very stable toward fragmentation and do not dissociate when injected into helium with kinetic energies of up to 350 eV. We have performed some fragmentation studies of  $\text{LaC}_{44}^+$  and larger  $\text{LaC}_{2n}^+$  clusters in neon buffer gas, where collisional excitation of the cluster cations is substantially more efficient than in helium. The fragmentation patterns of these larger  $\text{LaC}_{2n}^+$  clusters are very similar to those observed for  $\text{M}@\text{C}_{2n}^+$  fullerenes by other authors:<sup>14</sup> the clusters are reduced by the sequential loss of  $\text{C}_2$  units until they reach a critical size ( $\text{LaC}_{40}^+$  in our experiments) and then dissociate by losing  $\text{LaC}_4^+$  and other small  $\text{LaC}_{2n}^+$  fragments. Large  $\text{LaC}_{2n+1}^+$  fullerenes dissociate at much lower injection energies than the  $\text{LaC}_{2n}^+$  fullerenes by losing  $\text{C}_{2m+1}$  ( $m \geq 0$ ) fragments and forming stable even-numbered metallofullerenes.

## Discussion

**I. Structural Assignments. I.A. Ring Ia.** The two major pieces of information that we use in our structural assignments of the observed isomers are their measured mobilities and the variations in their abundances with cluster size. The mobilities of  $\text{LaC}_n^+$  ring Ia isomers are 9–16% smaller than the mobilities of the  $\text{C}_n^+$  isomer believed to be a monocyclic carbon ring<sup>20</sup> (see Figure 2). A metal atom can increase the physical size of a carbon ring by being inserted into the ring (structure A in Figure 9) or by being attached to the outside of the ring, either directly (structures B and D) or through a chain of carbon atoms (structure C). In all four cases (A–D), we assume that the  $\text{La}^+$  ions form two covalent bonds with the carbon atoms in the cluster. In pure carbon rings with an even number of carbon atoms the four valences of each carbon atom can be satisfied by either alternating single and triple bonds (polyyne structure)

**TABLE 2: Geometrical Parameters of Small La-Containing Molecules (Optimized at the Hartree-Fock Level with DZP Quality Basis Sets)**

molecule	La-C bond length, Å	C-La-C bond angle, deg
La(CH <sub>3</sub> ) <sub>2</sub> <sup>+</sup>	2.43	103.5
LaC <sub>2</sub> H <sub>2</sub> <sup>+</sup> <sup>a</sup>	2.29	33.8
LaCH <sub>2</sub> <sup>+</sup>	2.11	
La(CH <sub>3</sub> ) <sub>2</sub> CH <sub>2</sub> <sup>+</sup>	2.86 <sup>b</sup>	93.9 <sup>c</sup>

<sup>a</sup> Bridged complex (C<sub>2v</sub> symmetry). <sup>b</sup> Bond distance to the carbon atom coordinated to two hydrogen atoms. <sup>c</sup> Bond angle between a carbon atom coordinated to three hydrogen atoms, La, and the carbon atom coordinated to two hydrogen atoms.

or consecutive double bonds (cumulene structure). The presence of a covalently bound dopant atom imposes restrictions on the bonding in a carbon ring. In all four structures (A, B, C, and D in Figure 9) the divalent La<sup>+</sup> forces the ring to assume a polyene geometry. The propagation of alternating single and triple bonds around the ring for structures A, B, and C is possible only if the cluster contains an even number of carbon atoms. In contrast, the propagation of polyene bonding around the ring in structure D requires an odd number of carbon atoms. Since we observe that ring Ia is favored for LaC<sub>2n</sub><sup>+</sup> clusters, structures A, B, and C seem to be the most plausible candidates.

To further evaluate the proposed structures, we have estimated their mobilities in helium buffer gas. The reduced mobility from momentum transfer theory is given by<sup>32</sup>

$$K_0 = \frac{(18\pi)^{1/2}}{16} \left[ \frac{1}{m_1} + \frac{1}{m_B} \right]^{1/2} \frac{e}{(k_B T)^{1/2}} \frac{1}{\sigma N} \quad (3)$$

In this expression  $m_1$  and  $m_B$  are the masses of the ion and the buffer gas, respectively,  $N$  is the buffer gas number density, and  $\sigma$  is the average collision cross section. The collision cross section is calculated by averaging over all possible orientations of the cluster in space, assuming hard sphere interactions. A recent comparison of mobilities calculated using hard sphere interactions to those determined from trajectory calculations with a more realistic 4-6-12 potential suggests that the hard sphere approximation should be accurate to within a couple of percent for a family of similar isomers.<sup>38</sup> To estimate the collision cross section, one needs to know the geometry of the cluster and two empirical parameters: the hard sphere collision distances for C-He and La-He collisions. The geometries of most carbon clusters considered in this work were optimized in quantum chemical calculations at the MNDO level. La-C bond distances and bond angles were determined in *ab initio* calculations for small model systems. These calculations were performed at the Hartree-Fock level with the basis sets of double- $\zeta$ -polarized quality and 11-electron relativistic effective core potential on La<sup>39</sup> using the Gaussian-92 program.<sup>40</sup> The model systems and their optimized geometric parameters are listed in Table 2. The hard sphere distances for C-He collisions were determined by fitting mobility data for pure carbon clusters, and an average value of 2.73 Å was used. The La-He hard sphere collision distance is taken to be 3.07 Å, as determined from the measured mobilities of La<sup>+</sup> and La<sub>2</sub><sup>+</sup>.

The estimated mobilities of structures A, B, C, and D are plotted in Figure 9 along with the measured mobilities of ring Ia. In the mobility estimates for structures A, B, and C (and D) we used La-C bond lengths and bond angles determined in *ab initio* quantum chemical calculations for La(CH<sub>3</sub>)<sub>2</sub><sup>+</sup>, LaC<sub>2</sub>H<sub>2</sub><sup>+</sup>, and LaCH<sub>2</sub><sup>+</sup>, respectively (Table 2). It is clear from Figure 9 that the mobilities of all four structures are close to the measured mobilities of ring Ia, and structure A gives the best fit.

An estimate of the La<sup>+</sup>-C<sub>n</sub> bond energies for structures A-C can be obtained from bond additivity concepts using the measured energies of La<sup>+</sup>-C bonds (2.39 eV for a single and 4.26 eV for a double bond<sup>41</sup>) and average carbon-carbon bond energies (3.6 eV for a single, 6.3 eV for a double, and 8.7 eV for a triple bond<sup>42</sup>). The energy gain associated with the formation of structures A, B, and C from a La<sup>+</sup> ion and a monocyclic C<sub>2n</sub> ring is then estimated to be 1.2, 2.4, and 1.9 eV, respectively. For small LaC<sub>n</sub><sup>+</sup> rings the strain energy, which results from a substantial deviation of C-C-C bond angles from their ideal values of 180° for sp-hybridized carbon atoms, becomes an important consideration.<sup>31</sup> The strain energy can be reduced by the rehybridization of some of the atoms in the ring (to obtain ideal bond angles less than 180°) or by incorporation of additional atoms into the ring. The first way of strain reduction is common to all proposed ring Ia structures, while the second is unique to structure A. Since the La-C bond is approximately 1.8 times longer than an average C-C bond, insertion of La<sup>+</sup> into a carbon ring is almost equivalent to incorporation of three carbon atoms in terms of the strain reduction. The strain energy reduction in a LaC<sub>n</sub><sup>+</sup> ring resulting from the insertion of the La<sup>+</sup> is estimated to be around 2.2 eV for  $n = 10$  and around 1 eV for  $n = 20$ . Since the strain energy reduction for structure A is expected to be the largest, this structure for small LaC<sub>2n</sub><sup>+</sup> rings may be significantly more stable relative to structures B and C than suggested by the estimate above. For small LaC<sub>2n+1</sub><sup>+</sup> rings, strain reduction is also expected to stabilize structure A relative to structure D, and thus structure A may account for LaC<sub>2n+1</sub><sup>+</sup> ( $2n + 1 = 5-11$ ) ring Ia isomers as well. In summary, structure A seems to be the best candidate for small LaC<sub>n</sub><sup>+</sup> ring Ia isomers, while for larger LaC<sub>2n</sub><sup>+</sup> rings Ia structure B may be a plausible alternative.

*I.B. Ring Ib.* As can be seen from Figure 2, the mobilities of the ring Ib isomers of LaC<sub>n</sub><sup>+</sup> are 9-16% larger than those of the ring Ia isomers. The mobilities of the ring Ib isomers are also very close to the mobilities of the C<sub>n</sub><sup>+</sup> isomer attributed to a monocyclic ring, especially for  $n \geq 25$ . A metal atom has the smallest effect on a ring's mobility if it is located inside the ring (as in structure E in Figure 9). The La<sup>+</sup> ion located inside a carbon ring can be bound to the ring covalently, as pictured in Figure 9. In the bonding arrangement shown in the figure the ring is part polyene and part cumulene and has the two dangling bonds required to form a stable covalently bound complex with an internal La<sup>+</sup> ion. Such a complex can be formed for both LaC<sub>2n</sub><sup>+</sup> and LaC<sub>2n+1</sub><sup>+</sup> clusters, and from bond additivity concepts it is expected to have a stability comparable to those of structures B and D for clusters with an even and odd number of carbon atoms, respectively. However, unlike structures A-D, where incorporation of the La<sup>+</sup> is expected to reduce the strain, in structure E an additional strain energy is induced by the presence of the metal atom. An additional stabilization of structure E, on the other hand, should result from the overlap of empty La d-orbitals (both  $\sigma$ - and  $\pi$ -) with the  $\pi$ -systems of the carbon ring and from the delocalization of the valence electrons of the metal over the ring, which creates a favorable electrostatic attraction between the La and the ring. These stabilization factors are similar to those believed to be responsible for the stability of endohedral metallofullerenes. Both stabilization factors are expected to be especially important for clusters around LaC<sub>13</sub><sup>+</sup>, where the ring is just large enough to accommodate the metal atom and both orbital overlap and the electrostatic attraction are especially strong. Indeed, LaC<sub>13</sub><sup>+</sup> is the smallest LaC<sub>n</sub><sup>+</sup> cluster where the ring Ib isomer completely dominates the drift time distribution, while LaC<sub>14</sub><sup>+</sup> is the only LaC<sub>2n</sub><sup>+</sup> cluster where the relative abundance of ring

Ib is larger than the relative abundance of ring Ia (see Figure 3). Since the electron affinities of  $\text{C}_{2n+1}$  rings are around 0.8 eV larger than those of  $\text{C}_{2n}$  rings,<sup>43</sup> the stabilization of structure E due to charge transfer should be larger in the  $\text{LaC}_{2n+1}^+$  clusters, resulting in larger relative abundances of ring Ib for clusters with an odd number of carbon atoms, as observed experimentally.

The calculated mobilities of structure E (the dashed-dotted line in Figure 9) are in good agreement with the measured mobilities for the ring Ib family of isomers. The calculated mobilities are very close to those for the monocyclic  $\text{C}_n^+$  rings because the distortion of the ring (in the way pictured in Figure 9) compensates for the presence of the metal atom.

If the metal atom is not located inside a carbon ring, then the ring has to be substantially distorted in order to have a mobility similar to that measured for the ring Ib isomers. For example, a monocyclic carbon ring coordinated to a small nonlinear La-containing carbon fragment (such as structure F in Figure 9) should have mobilities close to those observed for the ring Ib isomers. Structure F is a pyramidal coordination complex of a  $\text{LaC}_n^+$  ring (structure A) with a monocyclic  $\text{C}_{2m+1}$  ring (the latter can be thought of as a polyyne ring with a carbene-type defect). This structure should be favored for clusters with an odd number of carbon atoms, as is observed experimentally for ring Ib. The dotted line in Figure 9 shows the calculated mobilities of structure F. The La–C bond lengths and the C–La–C bond angles for this structure are taken from the *ab initio* calculations for  $\text{La}(\text{CH}_3)_2\text{CH}_2^+$  (see Table 2). The agreement between the measured mobilities of ring Ib and the calculated mobilities of structure F is very good for clusters with more than 16 carbon atoms, but poor for smaller ones. The mobilities of similar structures with different bonding between the carbon ring and a La-containing fragment may be in better agreement with the experiment. However, the general disadvantage of all structures of this type is that they do not seem to be able to explain the size dependence of relative abundances of ring Ia and ring Ib for  $\text{LaC}_{2n}^+$  clusters, especially the abnormally high abundance of ring Ib for  $\text{LaC}_{14}^+$ .

In a preliminary account of this work<sup>25</sup> we speculated that ring Ib may also be due to structures B and D. Although the calculated mobilities of these two structures (the dashed line in Figure 9) are close to the measured mobilities of the ring Ib isomers for clusters with 13–25 carbon atoms, a substantial discrepancy emerges for larger clusters. Thus, it seems unlikely that structures B and D can account for the ring Ib isomers over the entire size range. Overall, the most likely geometry of the ring Ib isomers is a carbon ring with the metal atom attached to the inside of the ring.

**I.C. Ring II.** The mobilities of the  $\text{LaC}_n^+$  ring II isomers are very close to the mobilities of the  $\text{C}_n^+$  isomer assigned to a roughly planar bicyclic ring<sup>20</sup> (i.e. two carbon rings fused together). Another feature common to  $\text{LaC}_n^+$  ring II and  $\text{C}_n^+$  bicyclic rings is that both can isomerize to form rings with smaller mobilities. In the  $\text{C}_n^+$  system this can be achieved, for example, by forming bicyclic rings through a [2+2] cycloaddition of two smaller rings, in which case a retro-[2+2] process will open the bicyclic ring into a monocyclic ring.<sup>31</sup> However, in case of the  $\text{LaC}_n^+$  system the ring II isomers containing an odd and an even number of carbon atoms isomerize into different products, namely, into ring Ib and ring Ia isomers, respectively. The ring II isomers do not show any pronounced odd–even variations in either mobility or abundance, which suggests that  $\text{LaC}_{2n}^+$  and  $\text{LaC}_{2n+1}^+$  rings II have similar structures. Thus, isomerization of  $\text{LaC}_{2n}^+$  and  $\text{LaC}_{2n+1}^+$  ring II isomers into ring Ia and ring Ib, respectively, implies that

the ring Ia and ring Ib isomers can interconvert relatively easily, as was suggested above.

Some possible ring II structures are shown in Figure 9 (structures G–I). The bonding between the carbon rings in these structures proceeds through the breaking of a  $\text{C}\equiv\text{C}$  bond in  $\text{C}_{2n}$  rings or the utilization of the nonbonding electrons of the carbene-type defect in  $\text{C}_{2n+1}$  rings. Structures G and H are formed through an association of two rings with an even number of carbon atoms and two rings with an odd number of carbon atoms, respectively, and are expected to be stable for  $\text{LaC}_{2n}^+$  clusters. Structure I is formed through an association of rings with an even and an odd number of carbon atoms and is stable for  $\text{LaC}_{2n+1}^+$  clusters. The calculated mobilities of all three structures (the dashed-double dotted line in Figure 9) are very close to each other and are in excellent agreement with the measured mobilities of ring II. In all three structures the carbon rings are tilted with respect to each other, resulting in a slightly higher mobility than that of the planar bicyclic  $\text{C}_n$  rings, the difference being compensated for by the presence of the metal atom. Isomerization of structure G into a less mobile ring can proceed directly through the breaking of the two internal  $\text{C}=\text{C}$  bonds, while structures H and I can easily convert into a planar transition state (reminiscent of structure G) through the 1,2-shift(s) of the La atom. Other geometries with a different type of fusion between smaller rings may have similar mobilities and may be considered as candidates for the ring II isomers.

**I.D. Graphite Sheets.** The mobilities of the  $\text{LaC}_n^+$  isomer we assign to metal-containing graphite sheets are 9–14% smaller than the mobilities of pure  $\text{C}_n^+$  graphite sheets (see Figure 2). The decrease in the mobility due to the presence of a metal atom should be the largest if the metal atom coordinates to carbon atoms on the edge of a graphite sheet. The dashed-dotted line in Figure 2 shows the mobilities of planar, roughly circular  $\text{LaC}_n^+$  graphite sheets calculated assuming that the metal atom is coordinated to two dangling bonds on the edge of the graphite sheet (the La–C bond length is 2.43 Å). The calculated mobilities are in reasonable agreement with the experimental results over the entire size range, although consistently slightly larger. The difference between the calculated and the experimental mobilities may be due, for example, to small changes in the shape of a graphite sheet induced by the presence of the metal atom. A geometry with the metal atom sitting on top of the graphite sheet seems less likely because the calculated mobilities for this structure are only slightly different from the mobilities of pure  $\text{C}_n^+$  graphite sheets (the solid line below the “graphite” experimental points in Figure 2).

**I.E. Metallofullerenes.** As described above, we observe two groups of  $\text{LaC}_n^+$  fullerene isomers with slightly different mobilities. The mobilities of the faster group of metallofullerenes differ from the mobilities of pure carbon fullerenes by no more than 1.5% over the entire size range ( $n = 34$ –90) (see Figure 2). The three basic types of metallofullerene structures are endohedral, exohedral, and networked metallofullerenes (i.e. metallofullerenes with a metal atom substituted for carbon atom(s) in the fullerene cage). Our mobility simulations show that the mobilities of both exohedral and networked structures are at least 5% smaller than the mobility of a  $\text{C}_n^+$  fullerene. Therefore, we assign the “fast”  $\text{LaC}_n^+$  metallofullerene isomer to an *endohedral*  $\text{La}@\text{C}_n^+$  structure. Endohedral metallofullerenes are observed for  $\text{LaC}_{34}^+$ ,  $\text{LaC}_{36}^+$ , and all larger clusters and are the only fullerene isomer present for all clusters larger than  $\text{LaC}_{37}^+$ .

The group of  $\text{LaC}_n^+$  metallofullerenes with smaller mobilities exist in the  $n = 29$ –37 size range, where the fullerene cage is expected to be too small to readily encapsulate the metal

atom.<sup>14,44</sup> We attribute the decrease in the fullerene mobilities in this size range to the formation of non-endohedral metallofullerenes. The odd–even variation in the relative abundance of the non-endohedral metallofullerenes (see Figure 4) suggests that metallofullerenes with an odd number of carbon atoms are more stable than their even-numbered neighbors. Pure  $C_n^+$  fullerenes with an odd number of carbon atoms have a defect site in the fullerene cage. It is likely that in the non-endohedral  $LaC_{2n+1}^+$  metallofullerenes the La atom occupies this defect site and becomes a part of the carbon network, stabilizing these species with respect to non-endohedral  $LaC_{2n}^+$  fullerenes. We therefore assign “slow”  $LaC_{2n+1}^+$  metallofullerenes to *networked* structures.

The *ab initio* quantum chemical calculations we have performed for networked  $LaC_{29}^+$  metallofullerene (formed by replacing a carbon atom at a junction of three five-membered rings of the  $D_{5h}$  isomer of  $C_{30}$  fullerene with the  $La^+$  ion) show that the La forms three almost equivalent La–C  $\sigma$ -bonds with an average length of 2.53 Å. Using this geometry, we have estimated the mobilities of networked  $LaC_n^+$  ( $n = 29–37$ ) metallofullerenes (the dashed line in Figure 2). The simulation predicts an average 7% mobility decrease compared to pure  $C_n^+$  fullerenes, close to the experimentally observed 8–12% decrease. In these mobility estimates networked  $LaC_n^+$  metallofullerenes with an even number of carbon atoms are simulated as  $C_{n+2}$  fullerene cages with two adjacent carbon atoms replaced with the  $La^+$  ion. Non-endohedral  $LaC_{2n}^+$  fullerenes could also be viewed as intact fullerene cages with the metal atom attached externally. The estimated difference in mobilities of these two structures is less than 1% and cannot be resolved in our experiments.

**II. Growth of  $LaC_n^+$  Clusters.** The isomers and isomerization processes observed for the  $LaC_n^+$  clusters are similar to those observed for pure  $C_n^+$  clusters.<sup>20,22,23</sup> Small  $LaC_n^+$  clusters appear to be metal-containing carbon rings (ring Ia and ring Ib). Coalescence of small  $LaC_n^+$  rings with pure carbon rings presumably results in the formation of ring II. Since both valence electrons of the  $La^+$  ion in  $LaC_n^+$  rings are normally used to form bonds with the carbon atoms in the ring, the metal ion is unable to form new bonds without breaking the existing ones. Consequently, the behavior of  $LaC_n^+$  rings II is similar to that of pure  $C_n^+$  bicyclic rings. In particular, they can isomerize into ring Ia and ring Ib isomers, providing a mechanism for ring growth. Activation energies for this isomerization are close to those for isomerization of pure bicyclic  $C_n^+$  rings, although slightly (by 0.2 eV) lower (see Table 1). Overall, the growth mechanism of  $LaC_n^+$  rings seems to be very similar to that of pure  $C_n^+$  rings.<sup>20,31</sup>

For  $LaC_n^+$  with more than 29 atoms, metal-containing graphite sheets and subsequently metallofullerenes become the dominant isomers. Since we observe no small (15–25 atoms) graphite sheets and no clusters that could be considered as direct fullerene precursors, but do observe isomerization of metal-containing carbon rings into carbon networks, it is reasonable to assume that ring isomerization is the major mechanism of fullerene and graphite sheet formation under our conditions (a similar conclusion has been reached for pure  $C_n^+$  clusters<sup>22,23</sup>). For  $LaC_n^+$  ( $n \geq 35$ ) clusters, metallofullerenes (and graphite sheets for the smaller clusters) are essentially the only products of ring isomerization. For pure carbon clusters both fullerenes and monocyclic rings are formed, and the monocyclic  $C_n^+$  rings are not easily converted into fullerenes. Apparently, the metal atom either stabilizes fullerenes and graphite sheets (or the

important intermediates involved in their formation) or lowers the activation barriers for their formation through ring isomerization.

Our estimates of the activation barriers for isomerization of  $LaC_n^+$  rings into metallofullerenes show that they are not lower than those in the  $C_n^+$  system (see Table 1). On the other hand, our studies of the  $NbC_n^{+27}$  and the  $ZrC_n^{+45}$  systems, similar to those described here, show that Nb and Zr do lower activation barriers for isomerization of rings into fullerenes by about 0.6 eV. This difference must be related to the inability of the  $La^+$  ion to activate carbon–carbon bonds due to the absence of nonbonding valence electrons.

Since the activation barriers for isomerization of  $LaC_n^+$  rings into fullerenes are not lower than those for  $C_n^+$  rings, the thermochemical stabilization of isomerization products and/or intermediates is the most likely reason for the observed enhancement. The first few critical steps in this isomerization process are expected to include a series of cyclizations necessary to form an initial network of hexagons and pentagons.<sup>23</sup> These cyclizations may result in a large increase in the strain energy of the system. As discussed above, a metal atom incorporated into a carbon ring can significantly relieve the strain energy of the ring and thus stabilize isomerization intermediates. This stabilization occurs at the early stages of the reaction and thus is expected to increase the isomerization efficiency into all final products (endohedral and non-endohedral metallofullerenes and graphite sheets) equally. Indeed, as can be seen from Figure 7, the efficiency of  $LaC_n^+$  ( $n \geq 35$ ) fullerene formation increases smoothly as a function of  $n$ , despite the substantial difference in the structures of the final products ( $LaC_{35}^+$  is a networked metallofullerene,  $LaC_{36}^+$  is an endohedral metallofullerene, and for  $LaC_{37}^+$  both fullerene isomers are present).

Another factor that may affect the efficiencies of  $LaC_n^+$  isomer interconversion is the influence of the metal atom on the ionization energies of different isomers. Because of the low (5.58 eV) ionization potential of La, the differences between the ionization energies of various  $LaC_n$  isomers are expected to be reduced compared to the  $C_n$  system. Unfortunately, no experimental data are available for the ionization energies of  $C_n$  ( $n = 30–40$ ) rings and fullerenes. The ionization energies of  $C_n$  ( $n = 20–24$ ) rings are 7.2–8.2 eV,<sup>46</sup> while the ionization energies of  $C_n$  ( $n = 48–60$ ) fullerenes are in the 7.2–7.6 eV range.<sup>47</sup> Since the ionization energies are expected to decrease with cluster size, one may expect the ionization energies of  $C_n$  ( $n = 30–40$ ) rings to be about 1 eV lower than those of the fullerenes in this size range. Thus, in the  $LaC_n^+$  ( $n = 30–40$ ) system, fullerenes may be stabilized relative to rings by about 1 eV compared to the  $C_n^+$  system. This additional stabilization may contribute to the enhancement of fullerene formation in  $LaC_n^+$  clusters.

Metallofullerenes and metal-containing graphite sheets are the competing products of the isomerization of  $LaC_n^+$  ( $n \geq 30$ ) rings. For clusters with 30–34 carbon atoms there is a substantial strain energy associated with fullerene formation, so that fullerenes and graphite sheets are thermodynamically competitive at high temperatures and  $LaC_n^+$  rings isomerize into both of them. As fullerenes grow larger, their strain energy decreases and they become substantially more stable than graphite sheets, and so the major fraction of the rings now isomerize to form fullerenes. This explains why the relative abundance of the graphite sheets never exceeds a few percent for pure carbon clusters.<sup>20,31</sup> Both  $C_n^+$  graphite sheets and fullerenes can presumably be formed through the isomerization of carbon rings.<sup>22</sup> However, in the  $n = 30–35$  size range, where graphite sheets are probably energetically competitive with

fullerenes, ring isomerization in the  $\text{C}_n^+$  system is inefficient, so that only very small amounts of both isomers are formed. For larger  $\text{C}_n^+$  clusters, where ring isomerization becomes more efficient, graphite sheets are substantially less stable than fullerenes, and essentially all the rings that isomerize form fullerenes.

Fullerene formation through the isomerization of large carbon rings is one of the plausible mechanisms of fullerene synthesis in arc generators.<sup>23</sup> From the enhancement of fullerene formation observed in the present work for the  $\text{LaC}_n^+$  system one might expect metallofullerene yields in these generators to be higher than yields of pure carbon fullerenes. However, metallofullerene yields are normally several times lower than yields of  $\text{C}_n$  fullerenes. While we cannot rule out the possibility that the enhancement we observe is to a significant extent related to the charge state of the clusters, there are alternative explanations for the apparent lack of this enhancement in arc generators. On one hand, the low metallofullerene yields in arc generators may be related to the low sticking probability of the metal atom to a carbon cluster. On the other hand, the enhancement of fullerene formation may actually occur for  $\text{LaC}_n$  clusters in the  $n = 30\text{--}40$  size range, but once these small metallofullerenes are formed, it is difficult for them to grow up to the 60–90 atom size range, where relatively stable metallofullerenes exist. Indeed, it has been argued that the low efficiency of fullerene formation for carbon clusters with less than 40 atoms is an important factor in accounting for the efficient growth of larger stable fullerenes, such as  $\text{C}_{60}$  and  $\text{C}_{70}$ .<sup>23</sup>

## Conclusions

Five main families of isomers are observed for  $\text{LaC}_n^+$  clusters. These include three families of ring isomers (ring Ia, ring Ib, and ring II), La-containing graphite sheets, and metallofullerenes. The ring Ia isomers dominate for clusters with an even number of carbon atoms, and the ring Ib isomers dominate for the odd-numbered clusters. Several plausible geometries with similar mobilities can be suggested for all of the ring isomers. The ring I isomers probably have the metal ion inserted into the carbon ring (ring Ia) or coordinated to the inside of the ring (ring Ib). The ring II isomers appear to be small  $\text{LaC}_n$  and  $\text{C}_m$  rings fused together. The isomers observed for  $\text{LaC}_n^+$  clusters are similar to those observed for pure carbon clusters. The most notable differences are the absence of the linear chain isomer for  $\text{LaC}_n^+$  clusters with  $n < 10$ , the appearance of two "slow" ring I isomers with odd–even oscillation in their abundances, and the substantial increase in the relative abundances of the fullerene and graphite sheet isomers for the  $\text{LaC}_n^+$  clusters.

Ion mobility measurements provide a direct method for determining the position of the metal atom in metallofullerenes. All  $\text{LaC}_n^+$  metallofullerenes with  $n > 37$  formed in our source are endohedral. Although this result strictly refers to only ionized species, we do not expect the charge state to influence the position of the metal atom in  $\text{LaC}_{2n}$  fullerenes (for  $\text{LaC}_{2n+1}$  fullerenes the networked isomer may be stabilized by the presence of an additional electron). For metallofullerenes with  $n < 38$  networked (and, perhaps, exohedral) metallofullerene isomers are observed.

Annealing studies show that the ring II isomers for  $\text{LaC}_{2n}^+$  and  $\text{LaC}_{2n+1}^+$  clusters isomerize into ring Ia and ring Ib isomers, respectively. The activation energies for these processes are similar to those for pure carbon clusters. It appears that the ring Ia and ring Ib isomers interconvert relatively easily. For clusters with around 30 carbon atoms, isomerization of the rings

into fullerenes and graphite sheets starts to become important. The graphite sheet is the main isomerization product for clusters with 30–34 carbon atoms, while for clusters with more than 38 atoms >90% of the rings are converted into metallofullerenes. Isomerization of the rings into fullerenes and graphite sheets is considerably more efficient for  $\text{LaC}_n^+$  than for pure carbon clusters. However, the activation energies for these structural interconversions in the  $\text{LaC}_n^+$  and  $\text{C}_n^+$  systems are similar.

**Acknowledgment.** We gratefully acknowledge the support of this work by the National Science Foundation (Grant No. CHE-9306900) and the Petroleum Research Fund (administered by the American Chemical Society).

## References and Notes

- (1) Kroto, H. W.; Heath, J. R.; O'Brien, S. C.; Curl, R. F.; Smalley, R. E. *Nature* **1985**, *318*, 162.
- (2) Heath, J. R.; O'Brien, S. C.; Zhang, Q.; Liu, Y.; Curl, R. F.; Kroto, H. W.; Tittel, F. K.; Smalley, R. E. *J. Am. Chem. Soc.* **1988**, *110*, 4464.
- (3) Bethune, D. S.; Johnson, R. D.; Salem, J. R.; de Vries, M. S.; Yannoni, C. S. *Nature* **1993**, *366*, 123.
- (4) Kratschmer, W.; Lamb, L. D.; Fostiropoulos, K.; Huffman, D. R. *Nature* **1990**, *347*, 354.
- (5) Chai, Y.; Guo, T.; Jin, C.; Haufler, R. E.; Chibante, L. P. F.; Fure, J.; Wang, L.; Alford, J. M.; Smalley, R. E. *J. Phys. Chem.* **1991**, *95*, 7564.
- (6) Iijima, S. *Nature* **1991**, *354*, 56.
- (7) Iijima, S.; Ichihashi, T. *Nature* **1993**, *363*, 603. Bethune, D. S.; Kiang, C. H.; de Vries, M. S.; Gorman, G.; Savoy, R.; Vazques, J.; Beyers, R. *Nature* **1993**, *363*, 605.
- (8) Ugarte, D. *Nature* **1992**, *359*, 707.
- (9) Johnson, R. D.; de Vries, M. S.; Salem, J. R.; Bethune, D. S.; Yannoni, C. S. *Nature* **1992**, *355*, 239.
- (10) Weaver, J. H.; Chai, Y.; Kroll, G. H.; Jin, C.; Ohno, T. R.; Haufler, R. E.; Guo, T.; Alford, J. M.; Conceicao, J.; Chibante, L. P. F.; Jain, A.; Palmer, G.; Smalley, R. E. *Chem. Phys. Lett.* **1992**, *190*, 460.
- (11) Soderhom, L.; Wurz, P.; Lykke, K. R.; Parker, D. H.; Lytle, F. W. *J. Phys. Chem.* **1992**, *96*, 7153. Park, C.-H.; Wells, B. O.; DiCarlo, J.; Shen, Z.-X.; Salem, J. R.; Bethune, D. S.; Yannoni, C. S.; Johnson, R. D.; de Vries, M. S.; Booth, C.; Bridges, F.; Pianetta, P. *Chem. Phys. Lett.* **1993**, *213*, 196.
- (12) Diederich, F.; Ertle, R.; Rubin, Y.; Whetten, R. L.; Beck, R.; Alvarez, M.; Anz, S.; Sensharma, D.; Wudl, F.; Khemani, K. C.; Koch, A. *Science* **1991**, *252*, 548.
- (13) Kikuchi, K.; Suzuki, S.; Nakao, Y.; Nakahara, N.; Wakabayashi, T.; Shiromaru, H.; Saito, K.; Ikemoto, I.; Achiba, Y. *Chem. Phys. Lett.* **1993**, *216*, 67.
- (14) Weiss, F. D.; Elkind, J. L.; O'Brien, S. C.; Curl, R. F.; Smalley, R. E. *J. Am. Chem. Soc.* **1988**, *110*, 4464.
- (15) McElvany, S. W. *J. Phys. Chem.* **1992**, *96*, 4935.
- (16) von Helden, G.; Hsu, M. T.; Kemper, P. R.; Bowers, M. T. *J. Chem. Phys.* **1991**, *95*, 3835.
- (17) See, for example, Tou, J. C.; Boggs, G. U. *Anal. Chem.* **1976**, *48*, 1351. Carr, T. W. *J. Chromatogr.* **1977**, *15*, 85. Hagen, D. F. *Anal. Chem.* **1979**, *51*, 870. Karpas, Z.; Cohen, M. J.; Stimac, R. M.; Wernlund, R. F. *Int. J. Mass Spectrom. Ion Processes* **1986**, *83*, 163.
- (18) For a recent review see: St. Louis, R. H.; Hill, H. H. *Crit. Rev. Anal. Chem.* **1990**, *21*, 321.
- (19) Spangler, G. E.; Carrico, J. P. *Int. J. Mass Spectrom. Ion Processes* **1983**, *52*, 267.
- (20) von Helden, G.; Hsu, M. T.; Gotts, N. G.; Bowers, M. T. *J. Phys. Chem.* **1993**, *97*, 8182.
- (21) Jarrold, M. F.; Constant, V. A. *Phys. Rev. Lett.* **1991**, *67*, 2994.
- (22) Hunter, J. M.; Fye, J. L.; Jarrold, M. F. *Science* **1993**, *260*, 784.
- (23) Hunter, J. M.; Fye, J. L.; Roskamp, E. J.; Jarrold, M. F. *J. Phys. Chem.* **1994**, *98*, 1810.
- (24) Clemmer, D. E.; Shelimov, K. B.; Jarrold, M. F. *Nature* **1994**, *367*, 718.
- (25) Clemmer, D. E.; Shelimov, K. B.; Jarrold, M. F. *J. Am. Chem. Soc.* **1994**, *116*, 5971.
- (26) Shelimov, K. B.; Clemmer, D. E.; Jarrold, M. F. *J. Phys. Chem.* **1994**, *98*, 12819.
- (27) Clemmer, D. E.; Hunter, J. M.; Shelimov, K. B.; Jarrold, M. F. *Nature* **1994**, *372*, 248. Clemmer, D. E.; Jarrold, M. F. To be published.
- (28) Jarrold, M. F.; Bower, J. E.; Creegan, K. J. *Chem. Phys.* **1989**, *90*, 3615. Jarrold, M. F.; Bower, J. E. *J. Chem. Phys.* **1992**, *96*, 9180.
- (29) Hunter, J. M.; Fye, J. L.; Jarrold, M. F. *J. Chem. Phys.* **1993**, *99*, 1785.

- (30) Hunter, J. M.; Jarrold, M. F. Unpublished results.
- (31) Shelimov, K. B.; Hunter, J. M.; Jarrold, M. F. *Int. J. Mass Spectrom. Ion. Processes* **1994**, *138*, 17.
- (32) McDaniel, E. W.; Mason, E. A. *Transport Properties of Ions in Gases*; Wiley: New York, 1988.
- (33) Hunter, J. M.; Fye, J. L.; Jarrold, M. F. *J. Phys. Chem.* **1993**, *97*, 3460.
- (34) Jarrold, M. F.; Honea, E. C. *J. Phys. Chem.* **1991**, *95*, 9181.
- (35) Uggerud, E.; Derrick, P. J. *J. Phys. Chem.* **1991**, *95*, 1430.
- (36) Steinfeld, J. I.; Francisco, J. S.; Hase, W. L. *Chemical Kinetics and Dynamics*; Prentice-Hall: New Jersey, 1989.
- (37) Geusic, M. E.; Jarrold, M. F.; McIlrath, T. J.; Bloomfield, L. A.; Freeman, R. R.; Brown, W. L. *J. Chem. Phys.* **1987**, *86*, 3862.
- (38) Jarrold, M. F.; Hunter, J. M. To be published.
- (39) Ross, R. B.; Powers, J. M.; Atashroo, T.; Ermler, W. C.; LaJohn, L. A.; Christiansen, P. A. *J. Chem. Phys.* **1990**, *93*, 6654.
- (40) Frisch, M. J.; *et al.* *Gaussian-92*, revision E.1; Gaussian, Inc.: Pittsburg, PA, 1992.
- (41) Sunderlin, L. S.; Armentrout, P. B. *J. Am. Chem. Soc.* **1989**, *111*, 3845.
- (42) Lide, D. R., Ed. *Handbook of Chemistry and Physics*; CRC Press: Boca Raton, FL, 1993.
- (43) Yang, S.; Taylor, K. J.; Craycraft, M. J.; Conceicao, J.; Pettiette, C. L.; Cheshnovsky, O.; Smalley, R. E. *Chem. Phys. Lett.* **1988**, *144*, 431.
- (44) Guo, T.; Smalley, R. E.; Scuseria, G. E. *J. Chem. Phys.* **1993**, *99*, 352.
- (45) Shelimov, K. B.; Jarrold, M. F. To be published.
- (46) Bach, S. B. H.; Eyler, J. R. *J. Chem. Phys.* **1990**, *92*, 358.
- (47) Zimmerman, J. A.; Eyler, J. R.; Bach, S. B. H.; McElvany, S. W. *J. Chem. Phys.* **1991**, *94*, 3556.

JP950804E